→ Something to consider: change to missing momentum everywhere. Don't if it's too much work.

5

The Monojet Analysis

As has been described in Chapter 2, there are many searches for dark matter both at particle accelerators and elsewhere. At the LHC, one very promising channel is the so-called monojet search, where the detection of dark matter is done by looking for missing energy in association with one or more jets. The dark matter particles are expected to pass through the detector without leaving any signal since they are neutral and only interact very weakly. They can however be detected indirectly as missing energy when they recoil off one or more jets coming from initial state radiation.

First, the used physics objects are described in Section 5.1. Next, the selection of the events using the trigger is described in Section 5.2, and the subsequent event selection performed with fully reconstructed events is detailed in Section 5.3. The estimation of the background and the included systematic uncertainties are described Section 5.4 and 5.5, respectively. In Section 5.6, the obtained results are shown. The improvements achieved by going from the analysis strategy used in 2015 to the 2016 version are detailed in Section 5.7. Finally, the results are interpreted in terms of the considered dark matter models in Section 5.8.

5.1 Physics object reconstruction

While jets and missing transverse energy are evidently important objects in this analysis, other physics objects are used as well. Leptons and photons are for example vetoed in order to reject backgrounds, and are used to define the many control regions used for the background prediction.

consider not using subsubsection here, not really needed.

5.1.1 Jets

these

The method described in Section 4.3.7 is used to reconstruct the used PF jets, and the jet energy corrections are applied as well. Furthermore, the jets are required to have $p_T > 30\,\mathrm{GeV}$, and to pass the loose jet identification and pileup jet identification described in Section 4.3.7. Additionally, a jet cleaning is applied by requiring a jet charged hadron energy fraction CHF > 0.1 and a jet neutral hadron energy fraction NHF < 0.8. The jets are also tagged as b-jets using the Combined Secondary Vertex algorithm described in Section 4.3.8, with the loose working point.

reads as if all jets will be b-tagged

5.1.2 Missing transverse energy and hadronic recoil

In the signal region, the missing transverse energy E_T^{miss} is reconstructed as detailed in Section 4.3.10. For the control regions, the E_T^{miss} is redefined in order to imitate the E_T^{miss} shape in the signal region. This hadronic recoil U is obtained by removing the leptons or the photon present in the event from the E_T^{miss} computation.

like for photons (in 5.1.4), would be good to mention the veto purpose.

eg. "Loose identification criteria are used for the purpose of vetoing leptons." then the section can continue as is.

5.1.3 Leptons

Electrons are considered if they pass the loose electron selection, described in Section 4.3.3, and have $p_T > 10\,\mathrm{GeV}$ and $|\eta| < 2.5$. Similarly, muons are required to pass the loose muon identification described in Section 4.3.5 and to have $p_T > 10\,\mathrm{GeV}$ and $|\eta| < 2.4$. In the case of tau leptons, they are required to have $p_T > 15\,\mathrm{GeV}$ and $|\eta| < 2.3$. They should also pass the tau identification criteria, which require a jet with an identified subset of particles with a mass consistent with the decay products of a hadronic tau and which are isolated with a pileup corrected isolation cut requiring less than 5 GeV of energy deposits within a radial cone of $\Delta R < 0.3$.

The selection of electrons and muons for the control regions is however stricter they are required to pass the tight identification. "?"

5.1.4 Photons

Photons are required to have $p_T > 15\,\mathrm{GeV}$, $|\eta| < 2.5$, and to pass the loose identification criteria described in Section 4.3.3, in order to be considered for the photon veto. For the photon + jets control region, photons are required to pass the tight photon identification in order to be considered.

5.2 Trigger selection

In order to select events that have the monojet signature displayed in Figure 5.1, the trigger requires either $E_T^{miss} > 90\,\mathrm{GeV}$, where E_T^{miss} is the magnitude of the negative vectorial sum of the p_T of all particles at trigger level, or $H_T^{miss} > 90\,\mathrm{GeV}$, where H_T^{miss} is calculated as the magnitude of the negative vectorial sum of the momenta of all jets with $p_T > 20\,\mathrm{GeV}$. In order to avoid collecting events that contain noise signals coming from the detector, tight requirements are placed on the jets used in the H_T^{miss} computation. Jet energy corrections are already applied at the HLT-level and the jet NHF is required to be smaller than 0.9. Muons are not taken into account to compute E_T^{miss} and H_T^{miss}, so that the same trigger can be used to select the events for the muon control regions used for the background prediction.

efficiency → or: trigger is studied

Figure 5.1: Event display showing the monojet final state.

This trigger is evaluated using events passing the single electron trigger with a threshold of $p_T > 23\,\mathrm{GeV}$, and applying an extra offline selection requiring an electron with $p_T > 40\,\mathrm{GeV}$ passing the tight identification and a jet with $p_T > 100\,\mathrm{GeV}$ and $|\eta| < 2.5$. The trigger efficiency is computed by determining the fraction of events which additionally pass the signal triggers, as a function of the hadronic recoil. The efficiency is above 98% for events passing the analysis selection described in Section 5.3, as shown in Figure 5.2.

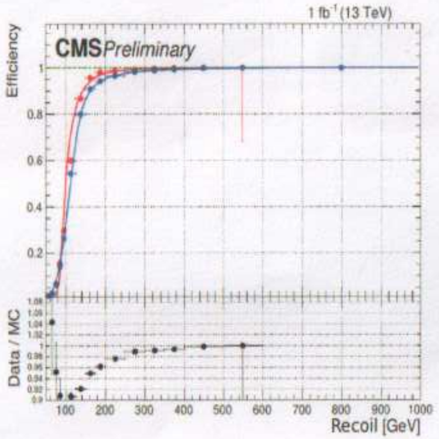

Figure 5.2: The efficiency of the used signal triggers as a function of the hadronic recoil, in MC (red) and data (blue).

To select events in ~~For~~ the electron control regions, a single electron trigger was used with a threshold at $p_T > 27\,\text{GeV}$. The efficiency of this trigger is determined as a function of p_T and η. This is done by "tagging" one electron with $p_T > 40\,\text{GeV}$ and $|\eta| < 2.1$ which passes the tight selection requirements. A second electron with $p_T > 10\,\text{GeV}$ and $|\eta| < 2.5$ is then selected, while ~~requiring~~ the invariant mass of this pair is required to be between 60 and 120 GeV, to correspond to the Z boson mass. This tag-and-probe method ensures that backgrounds are removed and allows to measure the efficiency by simply taking the fraction of probes that passes the single electron trigger. The obtained trigger-turn-on curves as a function of the electron transverse momentum are shown in Figure 5.3 for two η bins, covering the ECAL barrel and endcaps separately and leaving out the gap in between.

efficiency

Finally, the events in the photon control region are selected with a single photon trigger requiring an isolated photon with $p_T > 175\,\text{GeV}$. The performance of this trigger is measured in data selected using a single photon trigger with a lower p_T threshold, and the turn-on is shown in Figure 5.4.

It's not a gap really rather a poorly instrumented region

5.3 Event selection

Once the events have been fully reconstructed and the jets in the event have been corrected as described in Section 4.3.7, an event selection is applied in order to efficiently select signal events and reduce the contribution from backgrounds, such as the production of a leptonically decaying W boson in association with jets, semileptonic diboson decays, QCD multijets, and top quark production. The background contribution coming from events with a Z boson produced together with a number of jets, where the Z boson decays to two neutrinos, is irreducible as it produces exactly the same signature as the expected signal. The missing transverse energy E_T^{miss} is required to be larger than 200 GeV in order to be safely above the trigger turn-on. Additionally, the leading jet is required to have $p_T > 100\,\text{GeV}$, and $|\eta| < 2.5$. A cut on the difference in azimuthal angle between the E_T^{miss} and the first four leading jets of $\Delta\phi(jet, E_T^{miss}) > 0.5$ is also applied. This is done to suppress the QCD background from mismeasurements of jet momentum or detector noise, which would introduce missing transverse energy in the event,

most of the time, but we can also overmeasure

potentially add why

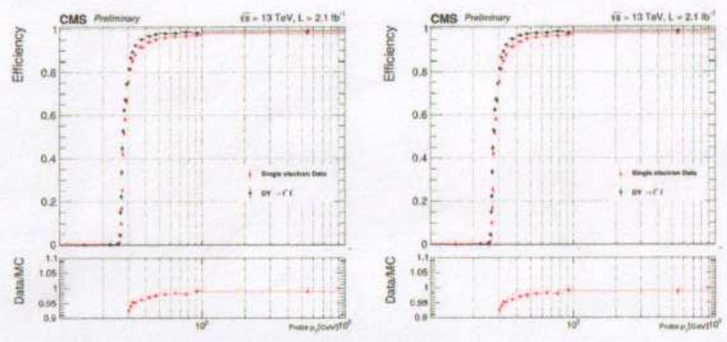

Figure 5.3: The efficiency of the single electron trigger in data (red) and MC (black) for $|\eta| < 1.4442$ (left) and $1.566 < |\eta| < 2.5$ (right).

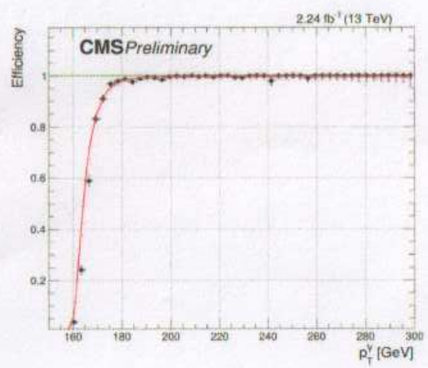

Figure 5.4: The efficiency of the single photon trigger measured in data.

in the same direction as the mismeasured jet. The events are further cleaned by applying quality filters to remove events coming from beam or instrumental backgrounds. Finally, events containing a lepton, a photon, or a b-jet are vetoed as well. Figure 5.5 shows the E_T^{miss} distribution for data and MC, after applying the described selection.

Events containing a lepton are vetoed to suppress the electroweak backgrounds, such as $W(l\nu)$ + jets and semileptonic diboson decays, while the photon veto is added to suppress the $Z(\nu\nu)$ + photon + jets and $W(l\nu)$ + photon + jets background processes, and to ensure there is no overlap with a similar dark matter search which investigates the final state consisting of missing energy and a photon. This rejects less than 1% of the signal. Finally, the b-jet veto reduces the background from events with a single top quark or top quark pairs by a factor 3 and only reduces the signal by 5 to 10%, depending on the type and mass of the mediator. No additional veto on the number of jets is applied.

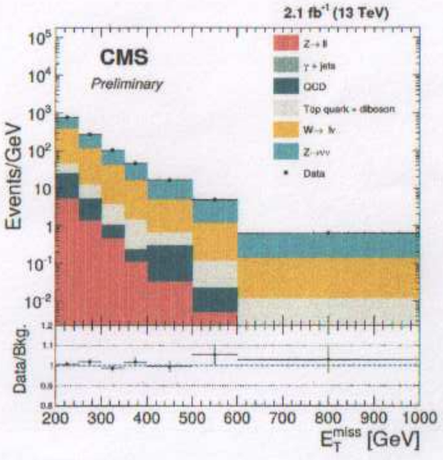

Figure 5.5: The missing transverse energy distribution after applying the described event selection, for data and MC.

This cannot be understood. You need first to be explicit on which control region is linked to which background for each R factor and recoil dependent?

5.4 Background estimation

The dominant background comes from events with a Z boson produced together with a number of jets, where the Z boson decays to two neutrinos. This produces the same signature of jets with missing energy as the signal, and results in an irreducible background. The second largest background consists of W + jets events with a leptonically decaying W boson. This background is already suppressed by the lepton veto, but a fraction of these events remain when the lepton is either not identified or outside of the detector acceptance. The remaining background events come from top quark decays, which are suppressed by the b-jet veto, semileptonic diboson (WW, WZ, and ZZ) decays, and QCD multijet events. The two main background contributions are estimated from five control regions in data consisting of dimuon, dielectron, single muon, single electron, and photon + jets events. The contributions from top quark decays and semileptonic diboson decays are estimated using simulated samples, while the QCD multijet background is estimated using a data-driven approach.

6→10 6 maybe non-obvious

5.4.1 The Z and W background estimation

The traditional control region for the Z boson background is the dimuon control region. This region is dominated by $Z \to \mu\mu$ events, which are very similar to the $Z(\nu\nu)$ + jets background events, the only difference being the decay mode. The production mode and kinematics in the control region are very similar, as well as the acceptance. However, the ~~branching ratio~~ of the Z boson into two muons is 6 times smaller than the branching ratio to two neutrinos. As a result, the dimuon control region contains about 10 times less Z boson events than the signal region. ~~In order~~ to improve this statistical limitation, other control regions have been added as well.

The yield of $Z(\nu\nu)$ and $W(l\nu)$ + jets events in the signal region is therefore estimated from five control regions by using the ratio between data and MC in the control region, per bin of the hadronic recoil distribution. For the prediction using $Z \to \mu\mu$ events in the dimuon control region for example,

notation does not correspond to Figure 5.6

explicitly define

the predicted yield of $Z \to \nu\nu$ events is given by

$$N_{Z(\nu\nu)} = \frac{N^{data}_{Z(\mu\mu)}}{N^{MC}_{Z(\mu\mu)}} N^{MC}_{Z(\nu\nu)} \tag{5.1}$$

$$= \frac{N^{data}_{\mu\mu} - N_{Bkgd}}{N^{MC}_{Z(\mu\mu)}} \cancel{N^{MC}_{Z(\nu\nu)}} \tag{5.2}$$

$$= \frac{N^{data}_{\mu\mu} - N_{Bkgd}}{\cancel{N^{MC}_{Z(\mu\mu)}}} \boxed{R_{Z(\mu\mu)\to Z(\nu\nu)}} \cancel{N^{MC}_{Z(\mu\mu)}}, \tag{5.3}$$

where the number of $Z(\mu\mu)$ + jets events in data $N^{data}_{Z(\mu\mu)}$ is given by the number events in the dimuon sample, removing the number of background events, and $N^{MC}_{Z(\mu\mu/\nu\nu)}$ represent the number of $Z(\mu\mu/\nu\nu)$ + jets events in MC. The transfer factors, denoted by R, are derived from simulation and take into account the impact of lepton acceptance and efficiency, as well as the additional E_T^{miss} requirement for the single electron control region. They also include the difference in branching ratio and the relation between the differential cross sections of the photon, W, and Z boson production as a function of the boson p_T. The transfer factors are computed as a function of the hadronic recoil, and are shown for the five different control regions in Figure 5.6. Furthermore, the Z/W ratio shown in the bottom right plot of Figure 5.6 provides an additional constraint since the single lepton control regions are also used to estimate the $Z(\nu\nu)$ + jets background.

NLO (repeat)

The simulated samples used for the background estimation are generated at leading order (LO) using the MADGRAPH generator, and corrected to next-to-leading order (NLO). These corrections are crucial in order correctly represent the data, since the simulation is approximately 40% higher than the data when using only LO calculations. The NLO QCD k-factors are derived from samples generated at NLO with MADGRAPH5_aMC@NLO, while the electroweak k-factors are obtained from theoretical calculations [130–133]. The differential cross section as a function of the boson p_T is shown in Figure 5.7 for photon, W, and Z production, and the obtained k-factors are displayed in the ratio plots. More details on the different control regions are given in the following.

Dimuon control region

In the dimuon control region the events are selected using the monojet triggers and applying the same requirements as described in Section 5.3 for the signal region, using the hadronic recoil instead of the missing transverse energy, except for the muon veto. Additionally, exactly two muons with opposite charge should be identified using the loose identification, and at least one should also pass the tight selection requirements. The leading muon should have a transverse momentum large than 20 GeV, and the second one should have $p_T > 10$ GeV. Finally, the dimuon mass should be between 60 and 120 GeV, corresponding to the Z boson mass.

Single muon control region

In order to model the second largest background, coming from $W(l\nu)$ + jets events, a single muon control region is used. This control region is in addition also used to constrain the $Z(\nu\nu)$ + jets background. The events in the single muon control region are required to pass the monojet triggers and event selection replacing the E_T^{miss} by the hadronic recoil obtained by removing the muon, except for the muon veto. One muon should then pass the tight selection requirements and have $p_T > 20$ GeV.

Dielectron control region

The dielectron control region is also used to constrain the $Z \to \nu\nu$ background. The events are selected by the single electron triggers. Similarly to the dimuon control region, the events are required to pass the monojet selection, except for the electron veto. Instead, exactly two electrons with $p_T > 10$ GeV are required to pass the loose identification described in Section 4.3.3. In addition, at least one electron should pass the tight selection requirements, and the leading electron is required to have $p_T > 40$ GeV in order to be consistent with the single electron trigger. Finally, the dielectron mass should be between 60 and 120 GeV, in order to be consistent with a Z boson